Evaluating mass spectrometry based hydroxyl radical protein footprinting of a benchtop Flash oxidation system against a synchrotron X-ray beamline.

Rohit Jain[1,2,3],* Nanak S. Dhillon[2,3],† Kanchustambham Vijayalakshmi[1,3], †† David T. Lodowski[2,3], Erik R. Farquhar[1,3], Janna Kiselar[2,3], Mark R. Chance[1,2,3]*

[1]Center for Synchrotron Biosciences, Case Western Reserve University, School of Medicine, 10900 Euclid Avenue, Cleveland, Ohio 44106, USA; [2]Center for Proteomics and Bioinformatics, Case Western Reserve University, School of Medicine, 10900 Euclid Avenue, Cleveland, Ohio 44106, USA; [3]Department of Nutrition, Case Western Reserve University, School of Medicine, 10900 Euclid Avenue, Cleveland, Ohio 44106, USA.

ABSTRACT: Hydroxyl radical protein footprinting (HRPF) using synchrotron X-ray radiation and mass spectrometry is a well-validated structural biology method that is providing critical insights into macromolecular dynamics. Numerous alternative sources for HRPF such as laser photolysis and plasma irradiation complement synchrotron-based HRPF. A recently developed commercially available instrument based on flash lamp photolysis, the Fox® system, enables access to laboratory benchtop HRPF. Here, we evaluate the feasibility of standardizing HRPF experiments in-house with a benchtop Fox® instrument as a precursor to synchrotron-based X-ray footprinting at the NSLS-II XFP beamline. Using lactate oxidase enzyme (LOx) as a model system, we carried out hydroxyl radical (•OH) labeling experiments using both instruments, followed by nanoLC-MS/MS bottom-up peptide mass mapping. Experiments were performed with high glucose concentrations to mimic highly scavenging conditions in biological buffers and human clinical samples, where less •OH are available for reaction with the biomolecule(s) of interest. The performance of the Fox® and XFP HRPF methods was compared, and we found that tuning •OH dosage enabled an optimum labeling coverage for both setups under physiologically relevant highly scavenging conditions. Our study demonstrates the complementarity of Fox® and XFP labeling approaches, showing that benchtop instruments such as Fox® photolysis system can increase throughput and accessibility of HRPF technology.

INTRODUCTION

Structural mass spectrometry (MS) methods including hydroxyl radical protein footprinting (HRPF), hydrogen deuterium exchange (HDX), native MS, ion-mobility MS and chemical cross-linking MS are yielding valuable complementary structural information to validate three-dimensional protein structures and track their structure and dynamics.[1-5] Amongst these, the HRPF technique has been instrumental for assessment of structures and interrelationships between proteins, higher order structure of proteins/protein complexes and examining protein-drug complexes.[6-7] HRPF assess macromolecular structure and dynamics by utilizing hydroxyl radicals (•OH) to label and probe the solvent-accessible side chains of proteins. •OH form irreversible covalent adducts with protein side chains dictated by solvent accessibility and intrinsic reactivity of side chains. After labeling, bottom-up proteomics approaches utilizing protease digestion and liquid chromatography (LC-MS/MS) coupled with mass spectrometry are routinely used to detect and quantify these modified protein side chains.[8] The rate of hydroxyl (OH) modification at peptide and residue levels changes for surface exposed amino acids in response to structural changes in the protein, enabling a readout of these changes in structure and dynamics. HRPF offers no size limitation, high-throughput experimentation and can be performed under physiologically relevant conditions for purified samples in buffer.[8-10] With these developments, HRPF has shown advantages in assessing macromolecular structure and dynamics over other low resolution structural biology techniques such as CD, fluorescence and SAXS, providing much needed structural insight which is complementary to high resolution techniques, such as cryo-EM and X-ray crystallography.[8, 11]

HRPF is an umbrella term for covalent labeling approaches employing •OH adducts, where the •OH can be generated by a variety of approaches - radiolysis of water by X-rays, gamma rays, electron beams, electric discharge or plasma source, decomposition of hydrogen peroxide (H_2O_2) using transition metal-based Fenton chemistry, and photolysis of H_2O_2 using lasers (FPOP) or a high pressure flash oxidation lamp.[12-18] Among these •OH sources, high intensity X-ray synchrotron beamlines continue to be essential resources for HRPF method development and its applications.[19-22] X-ray beamlines deliver a measurable, reproducible, and controlled •OH dose on microsecond to millisecond (and longer) timescales. The availability of high •OH dose at synchrotron beamlines for the structural biology community has allowed studies of complex and highly scavenging systems such as virus assembly, neurodegenerative diseases, epitope

mapping and time-resolved macromolecular dynamics.[23-26] Until now, MS analysis steps for X-ray irradiated samples have been carried out at a geographic separation from the synchrotrons resulting in a slow feedback loop between sample chemistry optimization, beamline experiment, and data analysis.[27] The availability of a benchtop OH labeling setup for worldwide MS facilities in conjunction with MS access at synchrotron X-ray beamlines could accelerate wider adoption of HRPF technology by the structural biology community.

A benchtop device for generation of •OH, the Flash oxidation (Fox®) Protein Footprinting System, has been recently commercialized by GenNext® Technologies.[17, 28-29] The Fox® system is a semi-automated protein oxidation system that uses a very brief (<10 µs FWHM) and very intense broadband UV output, to drive the generation of •OH from H_2O_2. The benchtop availability of •OH with Fox® can help standardize and design HRPF experiments in-house and compliment HRPF experiments at established synchrotron X-ray footprinting (XFP) beamlines. This collaborative approach can increase throughput and accessibility of HRPF technology. To provide this resource, we recently installed a Fox® Footprinting System in the Center for Proteomics and Bioinformatics at Case Western Reserve University. The method of generation of •OH, sample delivery and dosimetry workflows are entirely different for Fox® and XFP (Table 1). Specifically, Fox® uses a flash oxidation lamp to generate •OH from the UV photolysis of exogenously added H_2O_2. Changes in the photometric absorbance of an internal standard dosimeter, such as Adenine or Tris buffer, are measured, providing an estimation for the delivered •OH dose by real-time in-line radical dosimetry. In comparison, the 17-BM beamline at National Synchrotron Light Source II employs a 96-well high-throughput apparatus for performing X-ray exposures for water radiolysis, and optimizes •OH dosage using an Alexa488 fluorescence assay and a 96-well fluorescence plate reader to determine delivered •OH dose.[30] In a complementary approach, a liquid jet is being used to deliver sample with automated in-line Alexa488 fluorescence dose measurements at beamline 3.3.1 of the Advanced Light Source.[31-32]

Parameter	X-ray Footprinting (XFP)	Flash Oxidation (FOX®)
*OH generation	Water radiolysis	Peroxide photolysis
Mode of access	Synchrotron beamline	Benchtop box
Dosimetry analyte	Alexa488 fluorescence	Adenine UV absorbance
Quench conditions	Methionine amide	Catalase and Methionine amide

Table 1. A brief comparison of general parameters for 17-BM XFP beamline at NSLS-II and benchtop Fox® platform.

Due to the above differences, it is both timely and essential to compare the Fox® with the established XFP technique to enable wider implementation of HRPF technology. We have benchmarked the OH labeling of Fox® against a synchrotron XFP beamline using the lactate oxidase enzyme (LOx) as a model protein system. LOx was used for HRPF benchmarking due to its large size (167 kDa tetramer assembly) and our interests in wearable lactate biosensors for tracking hypoxia in airmen, fatigue monitoring in sports and sepsis in critical care.[33-38] "*In-operando*" protein footprinting experiments with clinical human samples can help in rational optimization of LOx constructs and sensor design for wearable lactate biosensor development. However, the •OH in HRPF readily react with components of human samples, like glucose, leading to undesirable secondary radical reactions and reduction of the total •OH concentration available for labeling reaction with the LOx enzyme.[30] As a proxy for the highly scavenging conditions in clinical human samples, we have used 2 different concentrations of glucose (2.5 mM and 10 mM) for our HRPF benchmarking study. The presented HRPF pipeline with complimentary Fox® and XFP OH labeling approaches will enable us to quickly optimize the new LOx constructs and accelerate the wearable lactate biosensor development. The benchmarking of the Fox® protein oxidation system to synchrotron X-ray beamlines will motivate the combination of different HRPF techniques. This collaborative approach will increase accessibility and throughput of the HRPF technology for addressing structural biology questions and accelerating higher order structural analysis for biopharmaceutical development.

METHODS

Materials. Flash Oxidation (FOX®) Protein Footprinting System and corresponding software for data collection and dosimetry analysis were purchased from GenNext® Technologies. Alexa Fluor™ 488 NHS Ester, dextrose (D-glucose) anhydrous, and 30% H_2O_2 were purchased from Fisher Scientific. Adenine and catalase enzyme (Bovine liver) were purchased from Sigma Aldrich. HPLC-grade acetonitrile and HPLC-grade water were purchased from Honeywell- Burdick & Jackson.

Recombinant LOx expression and purification. A synthetic vector construct consisting of a codon-optimized, N-terminally His-tagged *Aerococcus viridians* LOx construct was designed and synthesized (ATUM Bio, Newark, CA). *E. coli (BL21 (DE3)(pLysS))* were transformed with this vector and grown at 37 °C with shaking to an OD600 of 0.65 in a modified terrific broth mixture supplemented to 1 mM MgCl2, 0.5% glucose and 1.0% glycerol; upon achieving this value they were induced for 4 hours with 1 mM IPTG. Induced cells were harvested by centrifugation and frozen at -80 °C until purification. Frozen cells were ground under liquid nitrogen in a mortar and pestle to a fine powder prior to thawing by dilution in Lysis buffer (20mM HEPES pH 7.5, 100mM NaCl) supplemented with 0.5 mg/g cell paste of Lysozyme, two EDTA free protease inhibitor tablets (Roche) and Benzonase to reduce sample viscosity. Cells were then passed twice through a microfluidizer for lysis (typically 10,000 PSI). Supernatant was harvested by centrifugation 35,000 x g, 30 min) to separate the supernatant containing lactate oxidase from intact cells and cellular debris.

Supernatant was loaded onto a 5 mL Ni-NTA superflow column at a flow rate of 2 mL/min, column was washed with 50mL of high salt wash (20 mM HEPES 7.5, 300 mM NaCl, 10 mM imidazole), followed by 5 column volumes of low salt wash (20

mM HEPES 7.5, 100 mM NaCl, 10 mM imidazole). Lactate oxidase was then eluted from the column with elution buffer (20 mM HEPES 8.2, 100 mM NaCl, 300 mM imidazole) and 1 mL fractions collected. The elution fractions were analyzed by SDS-PAGE to check for protein quantity and purity. Fractions that exhibited LOX of high purity were pooled and concentrated to 10-15 mg/mL in an Amicon Ultra 15 100 kDa MWCO concentrator and further purified using gel filtration chromatography using 20mM HEPES pH 7.5, 100mM NaCl buffer to remove imidazole and low molecular weight impurities. Protein purity was assessed by SDS-PAGE and high purity (typically 95%) fractions were pooled and concentrated in an Amicon Ultra 15 100 kDa MWCO concentrator to a final concentration of 16 mg/mL. Pure LOx was frozen as 50 µL drops in liquid nitrogen and stored at -80 °C until further use. Prior to HRPF experiments, purified LOx (200 µl) was thawed and dialyzed against 1X PBS (200 mL) three times prior to labeling to remove HEPES buffer. After dialysis, the concentration of LOx was measured and stock solution was kept at +4 °C until further use. The stock LOx solution at ~66 µM (11 mg/ml) concentration was diluted to working LOx solution at 8 µM (1.3 mg/ml) concentration for labeling experiments. All concentrations were assessed with A280 measurements in a NanoDrop using an extinction coefficient of 205,360 $M^{-1}cm^{-1}$ for tetramer Lox assembly due to the nonstandard distribution of residues in the LOx sequence.[39]

Hydroxyl labeling with benchtop Fox® system. 2 µM LOx in 1X PBS (pH 7.4) samples were prepared with 50 mM H_2O_2, 1 mM Adenine, in varying scavenging glucose concentrations (0 mM, 2.5 mM, 10 mM) by reconstituting 8 µM LOx with 200 mm H_2O_2 (1X PBS) and 2 mM Adenine (1X PBS) just before labeling experiments. The samples (20 µl each at 2 µM LOx concentration) were injected separately into the Fox® benchtop labeling instrument and exposed at voltages of 0V, 500V, 600V, 700V, 800V, and 900V. A control LOx sample without H_2O_2 was injected to estimate background oxidation in LOx. OH labeled samples were collected in the fraction collector with collection tubes containing catalase (0.6 mg/ml) and methionine amide (60 mM) as a quencher solution (20 µl). The collected samples were immediately mixed manually to a final concentration of 0.3 mg/ml catalase and 30 mM methionine amide to break down remaining H_2O_2 and to quench secondary radicals. Quenched samples were then stored at -80 °C before MS analysis.

Hydroxyl labeling with X-ray exposures at 17-BM, NSLS-II XFP beamline. The working LOx solution at 8 µM (1.3 mg/ml) concentration was reconstituted with 1X PBS for labeling experiments. 2 µM LOx in 1X PBS (pH 7.4) samples, in varying scavenging glucose concentrations (0 mM, 2.5 mM, 10 mM), were first reconstituted with Alexa488 dye (to a final Alexa488 concentration of 4 uM) for determining appropriate X-ray dosage. Based on Alexa488 •OH dose response assay results, X-ray fluxes corresponding to beam powers (at 400 mA NSLS-II ring current) of 2.4 W, 15.2 W, and 32 W were chosen to overcome scavenging of 0 mM, 2.5 mM, and 10 mM glucose concentrations respectively, at exposure times of 0 ms, 12 ms, 20 ms, and 30 ms. Samples for Alexa488 dose response and mass spectrometry analysis were exposed in 5 µL volumes in 200 µL PCR tubes, with multiple replicates for each sample and exposure condition. OH labeled samples were immediately mixed with 60 mM methionine amide solution to a final concentration of 10 mM methionine amide to quench secondary radicals. Quenched samples were frozen in liquid nitrogen and shipped on dry ice to CWRU for mass spectrometric analysis.

MS sample preparation. Digested LOx samples were diluted with 0.1% formic acid and analyzed by a Waters nanoACQUITY UPLC coupled to a Thermo Orbitrap™ Eclipse Tribrid mass spectrometer. LOx peptides were desalted and concentrated using a Waters ACQUITY C_{18} trap column (100 Å, 5 µm, 180 µm * 20 mm) and eluted from a Waters ACQUITY C_{18} analytical column (100 Å, 75 µm, 250 mm). Two mobile phase systems - mobile phase A (0.1% FA in water) and mobile phase B (0.1% FA in Acetonitrile) were utilized to separate LOx peptides using a gradient from 0% to 40% B for 62 min at a flowrate of 300 nL/min and the capillary voltage of 2.1 kV. The gradient was then increased to 70% B from 62 to 66 min to allow the complete elution of LOx peptides from the analytical column. The C_{18} column was then washed with 98% B and re-equilibrated with 0% B solvent for 10 and 14 min respectively. Analytical column temperature was maintained at 40 °C. Full MS spectra were acquired in a positive polarity and the resolution was set to 120,000, with an AGC target of $4 * 10^5$ ions and maximum injection time was 50 ms.

Xcalibur software was used for manually extracting chromatograms and analyzing the modification of LOx peptides. In-house developed ProtMapMS software was also used to analyze dose response of LOx peptides in a semi-automated fashion.[40] OriginLab software was used to plot dose-response curve and calculate the modification rate for each modified peptide.

RESULTS

Comparison of dosimetry assays for XFP and Fox® platforms. Dosimetry assays have been developed to tune the •OH dose for comparing protein labeling in different experiments by assessing scavenging conditions in various biological buffers and purified samples. Both XFP (Alex488 fluorescence) and Fox® (Adenine dye/Tris buffer UV absorbance) platforms employ indirect dosimetry assays, where the change in fluorescence or UV absorbance due to destruction/modification of the dosimeter molecule is correlated to the •OH dose available for reaction with the biomolecule(s) of interest.[29-30, 41-42] In both strategies, the dosimeter reporter chemical is added to protein samples on the benchtop before conducting hydroxyl labeling experiments. However, these dosimetry assays and their procedures differ significantly for both Fox® and XFP platforms. Therefore, we first benchmarked each dosimetry assay for optimum hydroxyl labeling of LOx alone and in the presence of high glucose concentrations (2.5 mM and 10 mM).

For the XFP platform, the experimental conditions are first optimized using Alexa488 fluorescence loss and exposures are then repeated without added Alexa488 fluorescent dye for subsequent MS analysis. XFP experiments were performed using the 96-well high-throughput exposure device at the 17-BM beamline (NSLS II) for X-ray exposure followed by a direct readout of Alexa488 fluorescence in a 96-well plate reader and calculation of Alexa488 dose-response (D-R) rates.[30] The •OH yield for XFP at constant beam current is dependent on total

photon flux and was tuned by remotely changing aluminum attenuator thickness with the eight-position attenuator wheel. Alexa does-response rates of 20-80 s^{-1} have been determined experimentally to provide an optimal OH labeling without excessive sample destruction.

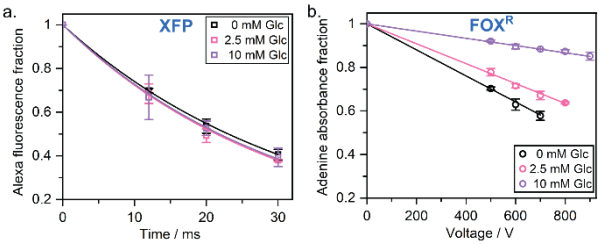

Figure 1. Indirect dosimetry for hydroxyl labeling of LOx samples on (a) XFP beamline (b) Fox® platform. The fraction of Alexa488 fluorescence (square) and Adenine UV absorbance (circle) was plotted for 0 mM glucose (black), 2.5 mM glucose (pink) and 10 mM glucose (purple) respectively. Points represent mean of data collected in duplicate and error bars represent ±1 SD. The loss of Alexa488 fluorescence from XFP platform was fitted to first-order reaction and calculated rate constants (s^{-1}) were used for comparison (Table 2). The change of Adenine UV absorbance from Fox® platform was fitted to linear function and calculated slopes were compared for comparison (V^{-1}) (Table 2).

We selected a high attenuation condition (using 762 µm thick aluminum) for labeling LOx in physiological conditions (1X PBS, pH 7.4) and at 0, 12, 20 and 30 ms time points. The modest X-ray power (2.4 W) and flux ($1.5*10^{14}$ photons/s) incident on LOx sample under this condition was considered adequate for OH labeling in physiological pH as the Alexa488 does-response rate for LOx in 1X PBS (30.5 s^{-1}, 762 µm) decreased significantly in comparison to 1X PBS alone (58 s^{-1}, 762 µm) due to scavenging by the protein itself. As expected, Alexa488 fluorescence decay for LOx under highly scavenging conditions with 2.5 mM glucose (3.2 s^{-1}, 762 µm Al) or 10 mM glucose (0.5 s^{-1}, 762 µm Al), was insignificant at high attenuation indicating the scavenging of •OH by the glucose. For experiments in the presence of glucose scavenger, we therefore increased available X-ray power by decreasing the aluminum attenuator thickness, selecting 152 µm Al for 2.5 mM glucose (15.2 W, $9.5*10^{14}$ photons/s) and 25 µm Al for 10 mM glucose (32 W, $20.0*10^{14}$ photons/s). We overcame glucose scavenging of •OH, yielding Alexa488 does-response rates of 38.7 s^{-1} for the 2.5 mM glucose condition and 32.4 s^{-1} for the 10 mM glucose condition.

In contrast to XFP, the change in dosimeter UV absorbance with the Fox® platform is essential to evaluating peptide modification rates obtained from MS. For the Fox® platform, samples pre-mixed with dosimeter (Adenine) and H_2O_2 are injected into a sample loop, which is connected to the fluidics module. Running buffer from the fluidics module pushes sample into the photolysis module, where broad-band UV (200-300 nm) light decomposes H_2O_2 into two •OH radicals as samples pass by a high-pressure Xenon flash lamp. The effective concentration of •OH is determined in real-time by a downstream dosimeter module by measuring the change in adenine absorbance at 265 nm. The •OH yield for the Fox® platform at constant H_2O_2 can be controlled by altering the voltage provided to the flash lamp. The decrease in Adenine absorbance (ΔAU) with increased lamp voltage at constant H_2O_2 provides a real-time parameter to tune the lamp voltage for optimum labeling. We used 50 mM H_2O_2 and multiple lamp voltages to label LOx under physiological pH (1X PBS, pH 7.4) and under scavenging conditions (2.5 mM and 10 mM glucose). At minimum voltage (500 V) the change in Adenine absorbance for LOx in the highest scavenging condition of 10 mM glucose (~14.9 AU) was much lower than physiological pH (~ 55.8 AU) and moderate scavenging at 2.5 mM glucose (~41.4 AU), indicating the scavenging of OH radicals by the glucose. The 50 mM H_2O_2 concentration was within recommended range (25 – 200 mM) and helped counter the •OH scavenging at higher scavenger concentration (10 mM glucose) where decrease in the Adenine UV absorbance was significantly lower than less scavenging conditions (0 mM and 2.5 mM glucose). The much lower Adenine absorbance change at 10 mM glucose concentration is noteworthy in comparison to XFP, where similar Alexa488 fluorescence decay rates were obtained for all physiological pH and scavenging conditions by increasing •OH dose with higher X-ray flux.

XFP parameters	**0 mM Glucose**	**2.5 mM Glucose**	**10 mM Glucose**
Alexa488 FL decay rate (s^{-1})	30.5	38.7	32.4
X-ray power* (W)	2.4	15.2	32
X-ray flux* (photons/s)	1.5 $*10^{14}$	9.5 $*10^{14}$	20.0 $*10^{14}$
Aluminum thickness (µm)	762	152	25
FOX® parameters	**0 mM Glucose**	**2.5 mM Glucose**	**10 mM Glucose**
Δslope# Adenine (V^{-1})	6.0 (0.1) $*10^{-4}$	4.6 (0.1) $*10^{-4}$	1.7 (0.1) $*10^{-4}$
ΔAbs## Adenine (mAU)	55.8	41.4	14.9

Table 2. Comparison of indirect dosimetry in physiological pH and scavenging conditions from XFP and Fox® platforms. *denotes X-ray power and flux incident on sample (at 400 mA NSLS-II ring current). # denotes slope of change in Adenine UV absorbance (265 nm) from Fox® platform after their fitting to linear function. ## denotes change in Adenine UV absorbance at 500 V from 0 V flash lamp voltage.

We labeled LOx samples using multiple lamp voltages and evaluated changes in Adenine absorbance with a linear function, to compare the effect of scavenging conditions on OH radical yield in the Fox® platform. We increased flash lamp voltage up to 900 V in order to overcome the high background scavenging of 10 mM glucose samples. A further increase in the Flash lamp voltage for higher •OH dosage was avoided due to oxygen bubble formation. As expected, the slope of Adenine decay for

Peptide	Sequence	k_{XFP} / s^{-1}	k_{FOX} /AU^{-1}
22-37	YIDVVNTYDL EEEASK	2.2 (0.1)	1.7 (0.2)
38-57	VVPHGGFNYI AGASGDEWTK	3.2 (0.1)	2.6 (0.1)
73-90	LAQDVEAPD TSTEILGHK	6.6 (0.1)	1.5 (0.1)
93-110	APFI**M**APIAA HGLAHTTK	4.0 (0.2)	10.8 (0.1)
156-168	DDQQNRD ILDEAK	17.1 (1.4)	5.2 (0.7)
162-168	DILDEAK	0.78 (0.01)	0.29 (0.04)
169-187	SDGATAIIL TADSTVSGNR	0.58 (0.02)	0.60 (0.08)
195-206	FVYPFG**M**PI VQR	9.1 (0.4)	-
210-225	GTAEG**M**SL NNIYGASK	13.6 (0.4)	-
232-247	DIEEIAGHS GLPVFVK	4.7 (0.3)	2.0 (0.1)
248-260	GIQHPEDA D**M**AIK	4.8 (0.4)	-
261-274	AGASGIW VSNHGAR	0.41 (0.10)	1.27 (0.07)
275-292	QLYEAPGSFD TLPAIAER	0.95 (0.02)	0.56 (0.01)
296-306	RVPIVFDSGVR	0.63 (0.02)	0.38 (0.02)
297-306	VPIVFDSGVR	1.27 (0.06)	0.55 (0.02)
354-367	V**M**QLTGSQNV EDLK	0.65 (0.20)	9.89 (0.34)
368-380	GLDLFDNPYG YEY	2.16 (0.08)	0.42 (0.01)

Table 3. Rate and corresponding fitting error (±) of hydroxyl modifications of LOx peptides on XFP and Fox® platforms in physiological pH (1X PBS, pH 7.4).

LOx in physiological pH (-6 $\Delta AU*V^{-1}$) was steeper than highly scavenging conditions, 2.5 mM glucose (-4.6 $\Delta AU*V^{-1}$) and 10 mM glucose (-1.7 $\Delta AU*V^{-1}$). The dosimeter assays for Fox® and XFP platforms provided guidance in selecting an optimal •OH dose for LOx samples. We subjected LOx samples to trypsin digestion and analyzed them with nanoLC-MS/MS to determine whether •OH dose in selected conditions was sufficient for OH labeling under physiological pH and scavenging conditions.

Comparison of LOx hydroxyl labeling on XFP and Fox® platforms. For benchmarking oxidative modifications, we performed a conventional bottom-up assessment of the OH labeled LOx samples from both XFP and Fox® platforms. Evaluation of the nanoLC-MS data obtained following trypsin digestion of LOx revealed similar ~67% labeling coverage of LOx protein sequence on XFP and Fox® platforms (SI Figure S2). The fraction of unmodified peptide was plotted against exposure time for XFP and modification rates were determined by fitting to a pseudo-first-order rate equation. For Fox®, the fraction of unmodified peptide was plotted against the change in UV absorbance at each flash lamp voltage and modification rates were determined by fits to a linear function. These modification rates provide a measure of the reactivity of a given region of the protein relative to other regions as well as in response to changes in either structure or total •OH dose. The modification rates for all modified LOx peptides in physiological pH (1X PBS) were tabulated (Table 3). LOx peptides differ in their inherent sensitivity to •OH, showing modification rates varying from low to high reactivity with the same reactivity trend observed on both XFP and Fox® platforms. Methionine-containing peptides show the largest OH reactivity among all LOx peptides on both HRPF platforms as dictated by the highest intrinsic reactivity pf methionine residue towards •OH.

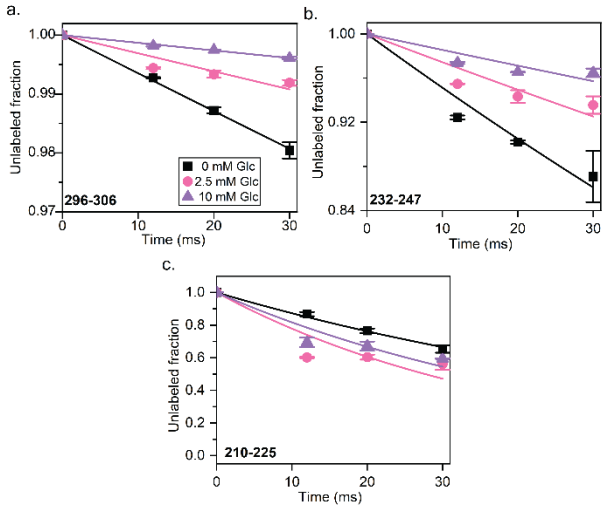

Figure 2. Hydroxyl modification of selected LOx peptides on XFP platform in physiological pH and scavenging conditions. (a) Low reactive peptide. (b) Moderate reactive peptide. (c) Methionine containing highly reactive peptide. The unlabeled fraction of peptides (filled symbols) at different exposure times was plotted for 0 mM glucose (black squares), 2.5 mM glucose (pink circles) and 10 mM glucose (purple triangles) respectively. Points represent mean of data collected in duplicate and error bars represent ±1 SD. The change in unlabeled peptide fraction from XFP platform was fitted to first-order reaction and rate constants (s^{-1}) were used for comparison (Table 4).

o compare the effect of scavenging conditions on OH labeling, we classified LOx peptides into low reactivity, moderate reactivity and methionine-containing high reactivity peptides. The dose response curves and rates of representative LOx peptides were then compared for all conditions (Figures 2-4, Table 4). The availability of •OH for protein modification decreases with

concomitant increase in scavenger concentration. As a result, the modification rate of a low reactive peptide (296-306) with the XFP platform decreased 2-fold with 2.5 mM glucose and 5-fold with 10 mM glucose (Figure 2, Table 4). A moderate reactive peptide (232-247) followed the same trend in the XFP platform showing 2-fold and 3-fold decreases in the presence 2.5 mM and 10 mM glucose respectively. In contrast, the modification rate of a typical methionine-containing highly reactive peptide (210-225) showed a 2-fold increase with 2.5 mM glucose, but then decreased slightly (~20%) with 10 mM glucose. The trend of Alexa488 modification rates in dosimetry assays for physiological pH and scavenging conditions follow that of methionine-containing highly reactive LOx peptide (Table 2). Hence, the relative increase of OH modification rates at higher scavenging conditions for methionine-containing peptides may be due to the high reactivity of methionine residue with respect to the scavenging compound and the availability of more •OH at higher-ray flux in XF experiments (Table 2).

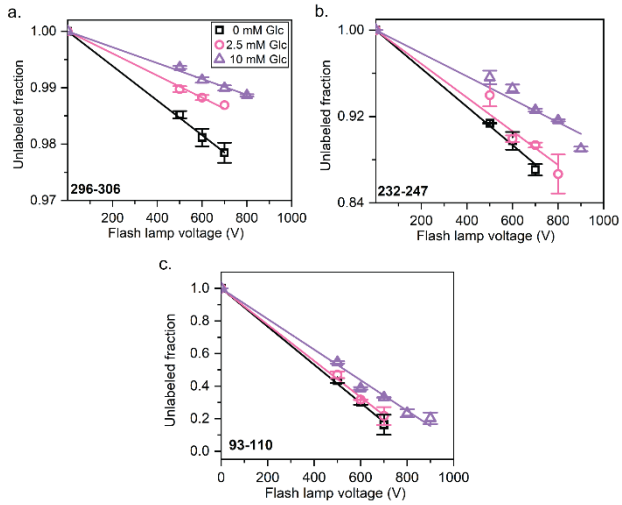

Figure 3. Hydroxyl modification of selected LOx peptides on Fox® platform in physiological pH and scavenging conditions vs. flash lamp voltage. (a) Low reactive peptide. (b) Moderate reactive peptide. (c) Methionine containing highly reactive peptide. The unlabeled fraction of peptides (empty symbols) with respect to exposed flash lamp voltages was plotted for 0 mM glucose (black squares), 2.5 mM glucose (pink circles) and 10 mM glucose (purple triangles) respectively. Points represent mean of data collected in duplicate and error bars represent ±1 SD. The change in unlabeled peptide fraction from Fox® platform was fitted to linear function and calculated slopes were compared for comparison (V^{-1}) (Table 4).

In analogous experiments with the Fox® platform, adenine UV absorbance decreased significantly for scavenging conditions (Table 2) and this made comparison of LOx peptides challenging (SI figure S3). We therefore plotted the unmodified fraction of LOx peptides against flash lamp voltage to better understand the dose-response of LOx peptides under scavenging conditions (Figure 3). Consistent with the above XFP results, the modification rates of low reactive (296-306) and moderate reactive (232-247) peptides decreased at higher scavenger concentrations on the Fox® platform (Table 4). However, the ratio of decrease in OH modification rates on the Fox® platform is lower than the XFP platform for both low reactive and highly reactive peptides. For e.g., the modification rate of low reactive (296-306) decreased ~2-fold and ~2.2-fold with 2.5 mM and 10 mM glucose respectively. The respective decrease in modification rate was lower for the moderate reactive (232-247) peptide, which did not decrease significantly with 2.5 mM glucose and decreased 1.6-fold with 10 mM glucose. The modification rate of methionine-containing high reactivity peptide (93-110) on Fox® platform decreased <10% with 2.5 mM glucose and ~20% at 10 mM glucose concentrations. In contrast to XFP, the dosimeter Adenine UV absorbance modification rates follow the trend of OH modification for differently reactive LOx peptides and show a continuous decrease from physiological pH to 2.5 mM glucose (1.3-fold) and 10 mM glucose (3.5-fold) concentrations. The decrease in modification rates for all peptides in the Fox® platform was therefore likely due to •OH quenching at higher scavenger concentration as the •OH dosage in the Fox® platform was constant for all experimental conditions.

k(XFP) / s^{-1}	**Sequence**	**0 mM**	**2.5 mM**	**10 mM**
296-306	RVPIVFD SGVR	0.65 (0.01)	0.31 (0.01)	0.13 (0.01)
232-247	DIEEIAGH SGLPVFVK	5.0 (0.3)	2.6 (0.2)	1.4 (0.1)
210-225	GTAEG**M**SL NNIYGASK	13.6 (0.4)	25.1 (3.1)	20.2 (1.7)
m#(FOX) /V^{-1}	**Sequence**	**0 mM**	**2.5 mM**	**10 mM**
296-306	RVPIVFD SGVR	0.26 (0.01)	0.17 (0.01)	0.12 (0.01)
232-247	DIEEIAGH SGLPVFVK	1.5 (0.1)	1.4 (0.1)	0.9 (0.1)
93-110	APFI**M**APIAA HGLAHTTK	11.7 (0.2)	11.1 (0.2)	9.4 (0.2)

Table 4. Comparison for hydroxyl modification rates of selected LOx peptides on XFP and Fox® platforms in physiological pH (0 mM Glucose) and scavenging conditions (2.5 mM and 10 mM Glucose). #denotes slope values (*10^{-4}) on Fox® platform.

Reduction of secondary oxidation of methionine containing peptides. We observed a large decrease in the unmodified fraction of two methionine containing LOx peptides (195-206 and 210-225) on the Fox® platform (Table 2). This large decrease was present even at low flash lamp voltages and was seen for both physiological pH and scavenging conditions (Figure 4a). For example, for peptide 210-225, the unmodified fraction at 500 V was ~3%, which is a large drop from our control experiments showing 88% unmodified at 0 V and 98% unmodified with no H_2O_2. The possibility of significant oxidation of methionine by freshly added H_2O_2 in the absence of UV radiation was therefore ruled out by control experiments. The oxidized samples post UV photolysis on the Fox® platform flow via in-line dosimetry module to fraction collector with collection tubes containing quencher solution. This ~7 min delay in

quenching on the Fox® platform is similar to high throughput XFP experiments at NSLS-II, where quencher solution is added post X-ray exposure on the 96-well high-throughput device and performed outside the X-ray experimental hutch.[30] We therefore attributed the observed large decrease in unmodified fraction of two methionine-containing peptides to the secondary oxidation of methionine residues in post-labeling conditions as the dose responses of methionine di-oxidation (+32 Da) were responsive to increase in scavenger concentrations.

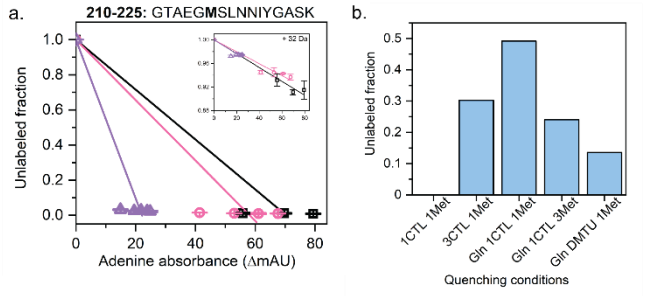

Figure 4. Change in post-labeling quenching conditions can significantly reduce the secondary oxidation of highly reactive Methionine containing peptide (210-225) in FOX® platform. (a) Fox® dose response of Methionine containing highly reactive peptide in physiological pH and scavenging conditions vs. adenine absorbance. The inset shows the unlabeled fraction for +32 Da modification on methionine residue. (b) The unlabeled fraction of 210-225 peptide at 800 V lamp voltage and 0 mM Glucose was plotted against different post-labeling conditions. The reagents in different quenching solutions in 1X PBS buffer include Catalase enzyme (1CTL = 0.3 mg/ml and 3CTL = 0.9 mg/ml), Methionine-amide (1 Met = 35 mM and 3Met = 105 mM), Glutamine α-amide hydrochloride (Gln = 5 mM) and N, N'-Dimethylthiourea (DMTU = 100 mM).

For the Fox® platform, catalase at 0.3 mg/ml concentrations is recommended in the quenching solution to degrade excess H_2O_2. Catalase has a large molecular weight (240 kDa) and increasing its concentration multifold can potentially hamper LC-MS sensitivity by increasing sample complexity and thus reduce footprinting resolution. Therefore, we employed different quenching conditions including a 3-fold higher concentration of catalase enzyme and compared secondary oxidation of LOx peptides (Figure 4b). We found that increasing the final catalase enzyme concentration to 0.9 mg/mL or adding glutamine amide (5 mM) with catalase (0.3 mg/ml) in methionine-amide (35 mM) containing quenching solutions markedly reduces the troublesome secondary oxidation of methionine-containing peptides on the Fox® platform. The adjusted quenching conditions did not decrease LC-MS S/N ratio at selected concentrations and did not affect post-labeling oxidation of moderate and low reactive peptides (SI figure S3). The improved quenching conditions in Fox® HRPF experiments could be used to quench the excess secondary radicals and significantly reduce the secondary oxidation of methionine-containing peptides.

DISCUSSION

The hydroxyl radical is an excellent chemical reagent for the structural characterization of proteins and enables single-residue resolution for validating structures and interactions or understanding the dynamics of structures in the context of ligand binding or assembly.[8] The advancements in recent years in throughput, automation, ease of use, and reliability of traditional HRPF labeling platforms including XFP and FPOP have facilitated its application to problems in protein structure, folding, and dynamics characterization.[6-8] The stability of covalent modifications in OH labeling allows HRPF to be combined with powerful bottom-up proteomics approaches and allows irradiated samples to be stored and re-analyzed after proteolysis. The stability of OH modifications provides a competitive edge for HRPF over its counterpart footprinting technique - hydrogen-deuterium exchange mass spectrometry (HDX-MS), where deuterium probes can exchange rapidly with protons in water. However, HRPF has not yet achieved the same level of uptake as HDX in the structural biology community and pharmaceutical industry. The commercial availability of an integrated and automated HDX-UPLC-MS system with inbuilt protein digestion and data analysis capabilities has greatly benefitted the routine characterization of protein dynamics, conformation and interactions.[43] Automation and integration in HRPF similar to HDX-MS will be crucial for its increased uptake and the availability of a benchtop Flash oxidation system is critical for such developments.

The benchtop HRPF labeling is now available as a commercial system with the Fox® platform and this advance in instrumentation represents a significant advancement for the footprinting field and the structural biology applications.[17, 28] One of these applications includes "*in-operando*" HRPF experiments for the molecular characterization of human biomarker-biorecognition element pairs, e.g., lactate-lactate oxidase enzyme (LOx), in clinical human samples. In this direction, we have benchmarked HRPF on the Fox® system with XFP for LOx in both physiological pH and scavenging conditions. Fox® differ significantly with standard XFP in the mode of generation of •OH, sample exposures and dosimetry procedures. Despite these differences, Fox® platform can provide consistent protein footprinting results similar to XFP. Overall, we found that OH labeling of LOx, a modest size protein (tetramer, 167 KDa), is comparable on both Fox® and XFP platforms. Further, peptides with differing OH reactivities can be labeled at both physiological pH and highly scavenging conditions (10 mM glucose). This implies that the benchtop Fox® protein oxidation system can complement HRPF at high flux X-ray sources and help in rational experimental design such as the optimization of LOx constructs.

On the other hand, we observed secondary oxidations resulting in and over labeling of methionine containing peptides on the Fox® platform due to high reactivity of methionine residue to •OH that could pose a challenge for HRPF experiments. These problems can be overcome by adding a higher concentration of catalase enzyme and glutamine amide in methionine-amide containing quenching solutions. However, the over labeling of methionine on existing HRPF platforms like XFP and FPOP has been a pertinent issue, reducing OH labeling coverage for methionine containing peptides unless oxidation conditions were carefully controlled.[21] Moving forward, the "camaraderie" framework outlined here could help develop •OH activated trifluoromethyl chemistry on the Fox® setup and bring its capability closer to XFP and FPOP platforms.[21, 44]

In summary, the Fox® protein oxidation system allows for FPOP-like HRPF experiments with real-time dosimetry in a safe, compact, and integrated benchtop platform. The commercial availability of semi-automated Fox® system could fasten the implementation of HRPF experiments at worldwide mass spectrometry resources. Fox® utilities for protein footprinting have been demonstrated by its use for determining the epitope of TNFα recognized by adalimumab antibody and measuring the effect of post-translational modifications in dynamic system like ovalbumin.[29, 45] Until now, the Fox® system applications have been *"in-vitro"* protein footprinting experiments in comparison to synchrotron X-rays and FPOP HRPF platforms, which have addressed a wide variety of structural biology questions for diverse macromolecules.[5, 7, 13, 20, 23-25] Though the Fox® system has the capability to address more challenging questions in future which range from *"in-cell"* protein footprinting to membrane proteins.[21, 23, 46-48] We envision that this benchmarking of the Fox® protein oxidation system in comparison to synchrotron X-rays under physiological pH and scavenging conditions will spur adoption of the Fox® system's HRPF applications and advance the HRPF field worldwide.

ASSOCIATED CONTENT

Supporting Information

Increase in glucose concentrations scavenges hydroxyl radicals and reduces decay of internal dosimeter fluorescence/UV absorbance (Figure S1, S-2), trypsin digestion of LOx revealed similar labeling coverage on XFP and Fox® platforms (Figure S2, S-3), hydroxyl modification of selected LOx peptides on Fox® platform in physiological pH and scavenging conditions vs. adenine absorbance (Figure S3, S-4), effect of different post-labeling quenching conditions in FOX® platform for LOx peptides (Figure S4, S-5), hydroxyl modification rates of selected LOx peptides on Fox® platform in physiological pH and scavenging conditions vs. adenine absorbance (Table S1, S-6).

The Supporting Information is available free of charge on the ACS Publications website.

SI Evaluation of MS based HRPF of benchtop Fox® against a synchrotron X-ray beamline (PDF)

AUTHOR INFORMATION

Corresponding Author

*Mark R. Chance - Center for Synchrotron Biosciences; Center for Proteomics and Bioinformatics; Department of Nutrition, Case Western Reserve University, School of Medicine, 10900 Euclid Avenue, Cleveland, Ohio 44106, USA.

*Email: mrc16@case.edu

*Rohit Jain - Center for Synchrotron Biosciences; Center for Proteomics and Bioinformatics; Department of Nutrition, Case Western Reserve University, School of Medicine, 10900 Euclid Avenue, Cleveland, Ohio 44106, USA

*Email: rxj298@case.edu

Present Addresses

†N.S.D. is presently a medical student at Northeast Ohio Medical University (NEOMED), Rootstown, OH, USA.

††K.V. is presently affiliated with Proteomics Center of Excellence, Northwestern University, Evanston, IL, USA.

Author Contributions

R.J., N.S.D. and D.T.L. prepared samples. R.J., N.S.D. and K.V. performed experiments and analyzed data with support from E.R.F. and J.K.. D.T.L., E.R.F. and J.K. contributed to editing the manuscript. R.J., N.S.D. and M.R.C. conceived the project, designed experiments, and wrote the manuscript. All authors have given approval to the final version of the manuscript.

Conflict of interest statement

The authors declare the following financial interests/personal relationships which may be considered as potential competing interests. M.R.C. is a Founder and Chief Scientific Officer of NeoProteomics, which provides access to footprinting technologies and services. J.K. is a consultant for NeoProteomics. M.R.C. owns shares and is a member of the scientific advisory board of GenNext® Technologies, Inc., makers of the benchtop flash oxidation system. CWRU acquired the FOX® system as part of normal research contracting (through federal funding). GenNext® Technologies did not financially contribute to this study.

ACKNOWLEDGMENT

This research was supported by the National Institutes of Health under R01-GM141078 and the Air Force Research Laboratory under agreement number FA8650-18-2-5402 (Case Number AFRL-2023-4823). Funding for development of the XFP beamline was provided by a Major Research Instrumentation award from the NSF (DBI-1228549) and Case Western Reserve University. This research used resources of the NSLS-II, a U.S. DOE Office of Science User Facility operated for the DOE Office of Science by Brookhaven National Laboratory under Contract No. DE-SC0012704. The DOE has established a portal for accessing X-ray footprinting beamlines at: https://berstructuralbioportal.org/x-ray-footprinting/

Disclaimer

This material is based on research sponsored by AFRL under agreement number FA8650-18-2-5402 (Case Number AFRL-2023-4823). The U.S. Government is authorized to reproduce and distribute reprints for Government purposes notwithstanding any copyright notation thereon. The views and conclusions contained herein are those of the authors and should not be interpreted as necessarily representing the official policies or endorsements, either expressed or implied, of AFRL or the U.S. Government.

REFERENCES

1. Sinz, A., Cross-Linking/Mass Spectrometry for Studying Protein Structures and Protein–Protein Interactions: Where Are We Now and Where Should We Go from Here? *Angewandte Chemie International Edition* **2018,** *57* (22), 6390-6396.

2. Jain, R.; Muneeruddin, K.; Anderson, J.; Harms, M. J.; Shaffer, S. A.; Matthews, C. R., A conserved folding nucleus sculpts the free energy landscape of bacterial and archaeal orthologs from a divergent TIM barrel family. *Proceedings of the National Academy of Sciences of the United States of America* **2021,** *118* (17).

3. Xu, G.; Chance, M. R., Hydroxyl radical-mediated modification of proteins as probes for structural proteomics. *Chemical reviews* **2007,** *107* (8), 3514-43.

4. Yassaghi, G.; Kukačka, Z.; Fiala, J.; Kavan, D.; Halada, P.; Volný, M.; Novák, P., Top-Down Detection of Oxidative Protein Footprinting by Collision-Induced Dissociation, Electron-Transfer Dissociation, and Electron-Capture Dissociation. *Analytical chemistry* **2022,** *94* (28), 9993-10002.
5. Liu, X. R.; Zhang, M. M.; Gross, M. L., Mass Spectrometry-Based Protein Footprinting for Higher-Order Structure Analysis: Fundamentals and Applications. *Chemical reviews* **2020,** *120* (10), 4355-4454.
6. Liu, X. R.; Rempel, D. L.; Gross, M. L., Protein higher-order-structure determination by fast photochemical oxidation of proteins and mass spectrometry analysis. *Nature Protocols* **2020,** *15* (12), 3942-3970.
7. Ralston, C. Y.; Sharp, J. S., Structural Investigation of Therapeutic Antibodies Using Hydroxyl Radical Protein Footprinting Methods. *Antibodies (Basel, Switzerland)* **2022,** *11* (4).
8. Chance, M. R.; Farquhar, E. R.; Yang, S.; Lodowski, D. T.; Kiselar, J., Protein Footprinting: Auxiliary Engine to Power the Structural Biology Revolution. *Journal of molecular biology* **2020,** *432* (9), 2973-2984.
9. Li, K. S.; Shi, L.; Gross, M. L., Mass Spectrometry-Based Fast Photochemical Oxidation of Proteins (FPOP) for Higher Order Structure Characterization. *Accounts of chemical research* **2018,** *51* (3), 736-744.
10. McKenzie-Coe, A.; Montes, N. S.; Jones, L. M., Hydroxyl Radical Protein Footprinting: A Mass Spectrometry-Based Structural Method for Studying the Higher Order Structure of Proteins. *Chemical reviews* **2022,** *122* (8), 7532-7561.
11. Jain, R.; Techert, S., Time-resolved and in-situ X-ray scattering methods beyond photoactivation: Utilizing high-flux X-ray sources for the study of ubiquitous non-photoactive proteins. *Protein and peptide letters* **2016,** *23* (3), 242-54.
12. Leser, M.; Chapman, J. R.; Khine, M.; Pegan, J.; Law, M.; Makkaoui, M. E.; Ueberheide, B. M.; Brenowitz, M., Chemical Generation of Hydroxyl Radical for Oxidative 'Footprinting'. *Protein and peptide letters* **2019,** *26* (1), 61-69.
13. Loginov, D. S.; Fiala, J.; Brechlin, P.; Kruppa, G.; Novak, P., Hydroxyl radical footprinting analysis of a human haptoglobin-hemoglobin complex. *Biochimica et biophysica acta. Proteins and proteomics* **2022,** *1870* (2), 140735.
14. Maleknia, S. D.; Brenowitz, M.; Chance, M. R., Millisecond Radiolytic Modification of Peptides by Synchrotron X-rays Identified by Mass Spectrometry. *Analytical chemistry* **1999,** *71* (18), 3965-3973.
15. Maleknia, S. D.; Downard, K. M., On-plate deposition of oxidized proteins to facilitate protein footprinting studies by radical probe mass spectrometry. *Rapid communications in mass spectrometry : RCM* **2012,** *26* (19), 2311-8.
16. Minkoff, B. B.; Blatz, J. M.; Choudhury, F. A.; Benjamin, D.; Shohet, J. L.; Sussman, M. R., Plasma-Generated OH Radical Production for Analyzing Three-Dimensional Structure in Protein Therapeutics. *Scientific reports* **2017,** *7* (1), 12946.
17. Sharp, J. S.; Chea, E. E.; Misra, S. K.; Orlando, R.; Popov, M.; Egan, R. W.; Holman, D.; Weinberger, S. R., Flash Oxidation (FOX) System: A Novel Laser-Free Fast Photochemical Oxidation Protein Footprinting Platform. *Journal of the American Society for Mass Spectrometry* **2021,** *32* (7), 1601-1609.
18. Shcherbakova, I.; Mitra, S.; Beer, R. H.; Brenowitz, M., Fast Fenton footprinting: a laboratory-based method for the time-resolved analysis of DNA, RNA and proteins. *Nucleic Acids Res* **2006,** *34* (6), e48.
19. Baud, A.; Aymé, L.; Gonnet, F.; Salard, I.; Gohon, Y.; Jolivet, P.; Brodolin, K.; Da Silva, P.; Giuliani, A.; Sclavi, B.; Chardot, T.; Mercère, P.; Roblin, P.; Daniel, R., SOLEIL shining on the solution-state structure of biomacromolecules by synchrotron X-ray footprinting at the Metrology beamline. *Journal of synchrotron radiation* **2017,** *24* (Pt 3), 576-585.
20. Gupta, S.; Sutter, M.; Remesh, S. G.; Dominguez-Martin, M. A.; Bao, H.; Feng, X. A.; Chan, L. G.; Petzold, C. J.; Kerfeld, C. A.; Ralston, C. Y., X-ray radiolytic labeling reveals the molecular basis of orange carotenoid protein photoprotection and its interactions with fluorescence recovery protein. *The Journal of biological chemistry* **2019,** *294* (22), 8848-8860.
21. Jain, R.; Dhillon, N. S.; Farquhar, E. R.; Wang, B.; Li, X.; Kiselar, J.; Chance, M. R., Multiplex Chemical Labeling of Amino Acids for Protein Footprinting Structure Assessment. *Analytical chemistry* **2022,** *94* (27), 9819-9825.
22. Kristensen, L. G.; Holton, J. M.; Rad, B.; Chen, Y.; Petzold, C. J.; Gupta, S.; Ralston, C. Y., Hydroxyl radical mediated damage of proteins in low oxygen solution investigated using X-ray footprinting mass spectrometry. *Journal of synchrotron radiation* **2021,** *28* (Pt 5), 1333-1342.
23. Du, Y.; Duc, N. M.; Rasmussen, S. G. F.; Hilger, D.; Kubiak, X.; Wang, L.; Bohon, J.; Kim, H. R.; Wegrecki, M.; Asuru, A.; Jeong, K. M.; Lee, J.; Chance, M. R.; Lodowski, D. T.; Kobilka, B. K.; Chung, K. Y., Assembly of a GPCR-G Protein Complex. *Cell* **2019,** *177* (5), 1232-1242.e11.
24. Mandel, I.; Ziv, D. H.; Goldshtein, I.; Peretz, T.; Alishekevitz, D.; Dror, A. F.; Hakim, M.; Hashmueli, S.; Friedman, I.; Sapir, Y.; Greco, R.; Qu, H.; Nestle, F.; Wiederschain, D.; Pao, L.; Sharma, S.; Moshe, T. B., BND-22, a first-in-class humanized ILT2-blocking antibody, promotes antitumor immunity and tumor regression. *Journal for ImmunoTherapy of Cancer* **2022,** *10* (9), e004859.
25. Siddiqi, M. K.; Kim, C.; Haldiman, T.; Kacirova, M.; Wang, B.; Bohon, J.; Chance, M. R.; Kiselar, J.; Safar, J. G., Structurally distinct external solvent-exposed domains drive replication of major human prions. *PLoS pathogens* **2021,** *17* (6), e1009642.
26. Tetter, S.; Terasaka, N.; Steinauer, A.; Bingham, R. J.; Clark, S.; Scott, A. J. P.; Patel, N.; Leibundgut, M.; Wroblewski, E.; Ban, N.; Stockley, P. G.; Twarock, R.; Hilvert, D., Evolution of a virus-like architecture and packaging mechanism in a repurposed bacterial protein. *Science (New York, N.Y.)* **2021,** *372* (6547), 1220-1224.
27. Farquhar, E. R.; Vijayalakshmi, K.; Jain, R.; Wang, B.; Kiselar, J.; Chance, M. R., Intact mass spectrometry screening to optimize hydroxyl radical dose for protein footprinting. *Biochemical and Biophysical Research Communications* **2023,** *671*, 343-349.
28. Weinberger, S. R.; Chea, E. E.; Sharp, J. S.; Misra, S. K., Laser-free Hydroxyl Radical Protein Footprinting to Perform Higher Order Structural Analysis of Proteins. *Journal of visualized experiments : JoVE* **2021,** (172).
29. Sharp, J. S.; Misra, S. K.; Persoff, J. J.; Egan, R. W.; Weinberger, S. R., Real Time Normalization of Fast Photochemical Oxidation of Proteins Experiments by Inline Adenine Radical Dosimetry. *Analytical chemistry* **2018,** *90* (21), 12625-12630.
30. Jain, R.; Abel, D.; Rakitin, M.; Sullivan, M.; Lodowski, D. T.; Chance, M. R.; Farquhar, E. R., New high-throughput endstation to accelerate the experimental optimization pipeline for synchrotron X-ray footprinting. *Journal of synchrotron radiation* **2021,** *28* (Pt 5), 1321-1332.
31. Gupta, S.; Chen, Y.; Petzold, C. J.; DePonte, D. P.; Ralston, C. Y., Development of Container Free Sample Exposure

for Synchrotron X-ray Footprinting. *Analytical chemistry* **2020,** *92* (1), 1565-1573.
32. Rosi, M.; Russell, B.; Kristensen, L. G.; Farquhar, E. R.; Jain, R.; Abel, D.; Sullivan, M.; Costello, S. M.; Dominguez-Martin, M. A.; Chen, Y.; Marqusee, S.; Petzold, C. J.; Kerfeld, C. A.; DePonte, D. P.; Farahmand, F.; Gupta, S.; Ralston, C. Y., An automated liquid jet for fluorescence dosimetry and microsecond radiolytic labeling of proteins. *Communications biology* **2022,** *5* (1), 866.
33. Hiraka, K.; Kojima, K.; Lin, C. E.; Tsugawa, W.; Asano, R.; La Belle, J. T.; Sode, K., Minimizing the effects of oxygen interference on l-lactate sensors by a single amino acid mutation in Aerococcus viridansl-lactate oxidase. *Biosensors & bioelectronics* **2018,** *103*, 163-170.
34. Hiraka, K.; Kojima, K.; Tsugawa, W.; Asano, R.; Ikebukuro, K.; Sode, K., Rational engineering of Aerococcus viridans l-lactate oxidase for the mediator modification to achieve quasi-direct electron transfer type lactate sensor. *Biosensors and Bioelectronics* **2020,** *151*, 111974.
35. Kiatamornrak, P.; Boobphahom, S.; Lertussavavivat, T.; Rattanawaleedirojn, P.; Chailapakul, O.; Rodthongkum, N.; Srisawat, N., A portable blood lactate sensor with a non-immobilized enzyme for early sepsis diagnosis. *Analyst* **2022,** *147* (12), 2819-2827.
36. Kim, J.; Campbell, A. S.; de Ávila, B. E.; Wang, J., Wearable biosensors for healthcare monitoring. *Nature biotechnology* **2019,** *37* (4), 389-406.
37. Leiros, I.; Wang, E.; Rasmussen, T.; Oksanen, E.; Repo, H.; Petersen, S. B.; Heikinheimo, P.; Hough, E., The 2.1 A structure of Aerococcus viridans L-lactate oxidase (LOX). *Acta crystallographica. Section F, Structural biology and crystallization communications* **2006,** *62* (Pt 12), 1185-90.
38. Terse-Thakoor, T.; Punjiya, M.; Matharu, Z.; Lyu, B.; Ahmad, M.; Giles, G. E.; Owyeung, R.; Alaimo, F.; Shojaei Baghini, M.; Brunyé, T. T.; Sonkusale, S., Thread-based multiplexed sensor patch for real-time sweat monitoring. *npj Flexible Electronics* **2020,** *4* (1), 18.
39. Wilkins, M. R.; Gasteiger, E.; Bairoch, A.; Sanchez, J. C.; Williams, K. L.; Appel, R. D.; Hochstrasser, D. F., Protein identification and analysis tools in the ExPASy server. *Methods in molecular biology (Clifton, N.J.)* **1999,** *112*, 531-52.
40. Kaur, P.; Kiselar, J. G.; Chance, M. R., Integrated Algorithms for High-Throughput Examination of Covalently Labeled Biomolecules by Structural Mass Spectrometry. *Analytical chemistry* **2009,** *81* (19), 8141-8149.
41. Roush, A. E.; Riaz, M.; Misra, S. K.; Weinberger, S. R.; Sharp, J. S., Intrinsic Buffer Hydroxyl Radical Dosimetry Using Tris(hydroxymethyl)aminomethane. *Journal of the American Society for Mass Spectrometry* **2020,** *31* (2), 169-172.
42. Huart, L.; Nicolas, C.; Hervé du Penhoat, M. A.; Guigner, J. M.; Gosse, C.; Palaudoux, J.; Lefrançois, S.; Mercere, P.; Dasilva, P.; Renault, J. P.; Chevallard, C., A microfluidic dosimetry cell to irradiate solutions with poorly penetrating radiations: a step towards online dosimetry for synchrotron beamlines. *Journal of synchrotron radiation* **2021,** *28* (Pt 3), 778-789.
43. Engen, J. R., Analysis of Protein Conformation and Dynamics by Hydrogen/Deuterium Exchange MS. *Analytical chemistry* **2009,** *81* (19), 7870-7875.
44. Cheng, M.; Guo, C.; Gross, M. L., The Application of Fluorine-Containing Reagents in Structural Proteomics. *Angewandte Chemie (International ed. in English)* **2020,** *59* (15), 5880-5889.
45. Cheng, Z.; Misra, S. K.; Shami, A.; Sharp, J. S., Structural Analysis of Phosphorylation Proteoforms in a Dynamic Heterogeneous System Using Flash Oxidation Coupled In-Line with Ion Exchange Chromatography. *Analytical chemistry* **2022,** *94* (51), 18017-18024.
46. Adilakshmi, T.; Soper, S. F.; Woodson, S. A., Structural analysis of RNA in living cells by in vivo synchrotron X-ray footprinting. *Methods in enzymology* **2009,** *468*, 239-58.
47. Cheng, M.; Zhang, B.; Cui, W.; Gross, M. L., Laser-Initiated Radical Trifluoromethylation of Peptides and Proteins: Application to Mass-Spectrometry-Based Protein Footprinting. *Angewandte Chemie International Edition* **2017,** *56* (45), 14007-14010.
48. Shortt, R. L.; Wang, Y.; Hummon, A. B.; Jones, L. M., Development of Spheroid-FPOP: An In-Cell Protein Footprinting Method for 3D Tumor Spheroids. *Journal of the American Society for Mass Spectrometry* **2023,** *34* (3), 417-425.